J. Indian Chem. Soc.,
Vol. 96, August 2019, pp. 1109-1116

Toxicity of pristine and β-cyclodextrin modified mesoporous alumina towards normal and cancer cell lines

Pritam Singh[a], Sanchaita Mondal[b], Moumita Saha[b], Krishna Das Saha[b]*, P. K. Maiti[c] and Kamalika Sen[a]*

[a]Department of Chemistry, [c]Department of Chemical Technology,

University of Calcutta, 92, Acharya Prafulla Chandra Road, Kolkata-700 009, India

E-mail: kamalchem.roy@gmail.com

[b]CSIR-Indian Institute of Chemical Biology, 4, Raja S. C. Mullick Road, Jadavpur, Kolkata-700 032, India

E-mail: chem.sanchaita@gmail.com, moumitasahaiicb@gmail.com, krishna@iicb.res.in

Manuscript received online 17 July 2019, revised and accepted 26 July 2019

Mesoporous alumina and its modifications are in vogue for their medical applications. These are mostly used for controlled delivery of different drugs for their internal porous configuration. However, studies on their candidature to be used for destruction of live cancer and normal cells are still in dearth. Herein, we report the synthesis and characterization of mesoporous alumina together with its modification using a carbohydrate, β-cyclodextrin (BCD). Thereafter we report on the cytotoxicity of these materials towards colon cancer cells (HCT 116) and normal kidney cells (HEK 293) together. The IC_{50} values of the pristine alumina and the BCD modified alumina were found to be 15.61 ng/mL and 23.39 ng/mL respectively for HCT 116. It has been observed that both the materials can be perceived to be potential reagents for destruction of cancer cells.

Keywords: Mesopororous alumina, β-cyclodextrin, HCT 116, HEK 293, cytotoxicity.

Introduction

An exponential growth of research in the field of nanotechnology especially mesoporous materials has been observed in the recent years. This trend of the modern science community towards mesoporous materials is quite obvious as these materials posses some unique properties such as high surface area, tunable pore size, higher stability, easy functionalization compared to that of the bulk materials. These properties make them novel and distinguished candidates for a variety of applications[1–4].

Alumina is one such candidate that has different applications in several branches of science. The most interesting property of such materials lies in their wear resistance capability and antimicrobial activity. Due to such properties, mesoporous alumina has found its application in the medical field as a ceramic material in the contemporary organ replacement therapy. In fact it has been used in hip joint prosthesis. It has also found applications in biochemical fields such as biosensors, protein separations, drug delivery, etc.[5–7].

However, the use of such candidates also results in their exposure to the living systems. Therefore, the impact of nanomaterials on biological systems has become mandatory[8] and has bred a new field of research known as "nanotoxicology". This term has captured our attention with the growth of their gradual penetration in industrial and social platforms[9].

Now a basic question arises regarding the reason behind such toxicity. A clear and an obvious answer to this query rely on the interaction between the nanomaterials and the cells of the living system. Particle size of such materials is anticipated to play a decisive role behind the extent of toxicity as smaller particles are likely to invade and penetrate the cell wall, enter into the cellular matrix, create an imbalance in the biochemical system therein causing cell damage[10].

Nanodimensional aluminum oxide shows numerous reports on toxicological assays in the literature[11]. Chen *et al.* reported that aluminium oxide nanoparticles reduced the cell viability of human brain microvascular endothelial cells by alteration in the potential of mitochondria[12]. The mechanism

also involved increased cellular oxidation, and decreased protein expression in presence of the particles. In another work Alshatwi *et al.* showed the cytotoxicity of Al_2O_3 nanoparticles towards human mesenchymal stem cells by changing the internal cellular structure. Altered gene expression factors were found to escalate the mitochondria mediated cell death[13].

β-Cyclodextrin (BCD) is a water soluble oligosaccharide with a toroid shape having glucopyranoside units linked by glycosidic bonds. The toroid has a lesser hydrophilic interior and a more hydrophilic exterior due to the spatial orientation of the -OH groups. This makes them good candidates to form inclusion complexes with drugs with a resultant advantage for controlled drug delivery due to enhanced solubility. BCD is also capable to penetrate body tissues and is known to have sufficient bioactivity to remove cholesterol from cultured cells. Additionally they are of wide interest because of their nontoxic behavior, as far as the *in vivo* studies are concerned. Therefore, BCDs are now well chosen in the field of drug delivery applications[14]. Rachmawati *et al*. reported BCD based drug delivery of curcumin to enhance its skin permeability[15]. In another work by Babbta and Agarwal, an inclusion complex of meloxicam in BCD to increase the dissolution rate of the drug was reported[16]. BCDs are also used to modify mesoporous materials for achieving targeted drug delivery. Recently in 2017, Abdous *et al.* developed a system based on BCD modified mesoporous silica for controlled loading and release of curcumin with higher cytotoxic efficacy for cancer cells[17]. Further, Zhang *et al*. reported BCD modified gold functionalized mesoporous silica for sustained release of 1-adamantaneacetic acid and fluorescein drug[18].

However, every such modification changes the toxicological features of the resultant species. The possibilities of altered toxicity of any chemical reagent at different chemical milieu should be considered and BCD is not an exclusion from this generalization. Rather, it should be considered more poignantly particularly because it has well known *in vivo* nontoxicity.

In this work we have prepared mesoporous alumina and modified it with a biopolymer β-cyclodextrin (BCD). We characterized these materials using different techniques like N_2 adsorption-desorption isotherm, FESEM (field emission scanning electron microscopy), TEM (transmission electron microscopy), and so on to get a clear idea about the surface and internal properties of these materials. The current scenario associated with the nanotoxicology directs us to go through a survey of the toxicity of such materials. So we have taken one human colon cancer cell (HCT 116) and a normal cell line (HEK 293 (Normal Human Epithelial Kidney) cells) to study the cytotoxicity of these materials.

Experimental

Materials:

Pluronic F-68 was purchased from Himedia Laboratory Pvt. Ltd. (India). Aluminium iso propoxide (98%) was purchased from Loba Chemie (Laboratory Reagents & Fine Chemicals) (India). β-Cyclodextrin (BCD) (98%) was purchased from Sisco Research Laboratories Pvt. Ltd. (India). Dulbecco's modified Eagle's medium (DMEM), Fetal Bovine Serum (FBS), antibiotic penicillin-streptomycin (PS), trypsin and ethylenediamine tetraacetic acid (EDTA) were purchased from Gibco BRL (Grand Island, New York, USA). 3-(4,5-Dimethylthiazol-2-yl)-2,5-diphenyltetrazolium bromide (45989, MTT-CAS 298-93-1-Calbiochem), dimethyl sulfoxide (DMSO), FlowCollect Annexin Red kit (Cat. No. FCCH100108) were bought from Merck-Millipore. Tissue culture plastic wares were bought from Genetix Biotech Asia Pvt. Ltd. All other chemicals were of AR grade and used as obtained.

Apparatus:

Quantachrome surface area analyzer instrument was used to get nitrogen adsorption-desorption isotherm at liquid nitrogen temperature (77 K). The field emission scanning electron microscopic images were obtained using JEOL JSM-7600F instrument. JEOL JEM 2100 HR with EELS transmission electron microscopy was used to get TEM images of the prepared materials. Perkin-Elmer FT-IR 783 spectrophotometer having resolution 1 cm^{-1} was used to get the Fourier transformed infra red (FTIR) spectra of the prepared materials in the range of 400 to 4000 cm^{-1} using KBr pellets. X-Ray diffraction (XRD) data was obtained from X-PERT-PRO Panalytical diffractometer. The data so obtained from XRD was then compared with the standard data obtained from the Joint Committee on Powder Diffraction Standards (JCPDS) software. A digital balance of Mettler Toledo, correct upto four decimal place was used to accurate weighing of the materials. Calcination was performed using Muffle furnace of Bysakh & Company, India instrument.

Synthesis of mesoporous alumina (MA):

The synthesis method was followed from a literature report[19]. Pluronic F-68 solution was prepared in ethanol in a beaker. In another beaker, aluminium isopropoxide was taken in ethanol and to complete the dissolution 3 mL of concentrated HNO_3 was added to the iso propoxide solution. In the next step, the iso-propoxide solution was mixed with pluronic solution under stirring condition. After 5 h of continuous stirring, the mixture was dried in an oven and finally the material was calcined at 1000°C for 4 h at a heating rate of 10°C/min.

Synthesis of BCD modified mesoporous alumina (BMMA):

For synthesis of BMMA, the water solution of BCD and ethanolic solution of iso propoxide were mixed with pluronic solution under stirring condition. As described above, after continuous stirring for 5 h, the mixture was dried in oven and finally calcined at 300°C for 4 h at the same heating rate as above.

Cell culture study:

The HCT 116 and HEK 293 cell lines were cultured in DMEM containing 10% FBS at 37°C in a humidified atmosphere under 5% CO_2. Cells were harvested with 0.5% trypsin and seeded at a required density to allow them to re-equilibrate a day before the start of experiment.

Cell viability assay:

The MTT assay was done to check the cell viability. HCT 116 and HEK 293 cells (1×10^6 cells/well) were plate in 96-well plate and treated with or without different concentrations of MA (4.46, 8.92, 17.84, 26.76 and 35.68 ng/mL) and BMMA (7.1, 14.2, 28.4, 42.6 and 54 ng/mL) for 24 h. Medium was discarded and MTT (4 mg/mL) was added to the wells and incubated for 3 h. After incubation, DMSO was added and the absorbance of the solution was measured at 595 nm using a micro plate reader.

Detection of apoptosis using fluorescence-activated cell sorting (FACS) analysis:

Apoptosis was assayed by using Annexin V fluorescein isothiocyanate (FITC) apoptosis detection kit as manufacturer's protocol with some modifications. HCT 116 cells treated with MA for 24 h and were stained with propidium iodide (PI) and annexin V-FITC. The percentage of live, apoptotic and necrotic cells were analyzed by BD LSRFortessa cell analyzer (Becton Dickinson, San Jose, CA, USA). Data from 10^6 cells were analyzed for each sample.

Characterization

N_2 adsorption-desorption analysis was performed to get surface information and pore size distribution of the solid samples. Barrett-Joyner-Halenda (BJH) method was applied to calculate the pore volume of the materials. Field emission scanning electron microscopy (FESEM) analysis was done using solid materials to take a clear view of the surface of the nanoparticles. Transmission electron microscopic (TEM) analysis was performed using a dispersed solution of the materials (prepared in water) to get a high resolution image of the surface and the particle size of the materials. The bond vibration data were recorded using FTIR spectroscopic method using solid samples. The crystalline nature of the prepared materials was confirmed form powder X-ray diffractometric technique using the solid form of the materials.

Results and discussion

N_2 Adsorption desorption analysis:

Both MA and BMMA show type II isotherm with H3 hysteresis loop (Fig. 1) characteristic for mesoporous adsorbent having slit shaped pores with plate-like assemblies[20–24]. The average pore diameter for MA and BMMA are ~10 and ~15 nm respectively (Fig. 1 inset). The BJH pore volumes for MA and BMMA are 0.080 and 0.030 cm^3/g.

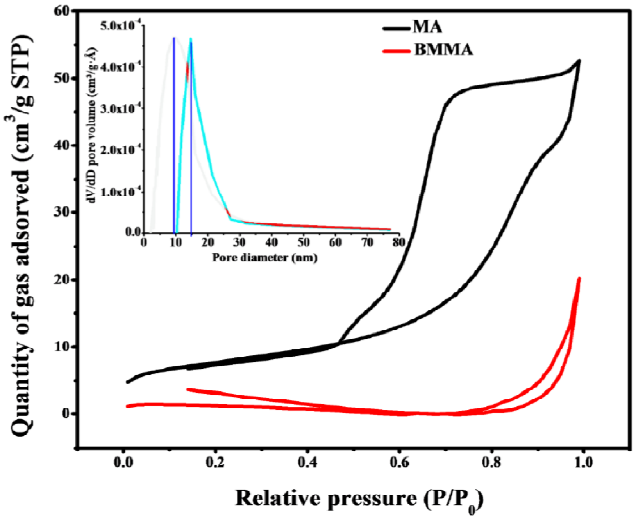

Fig. 1. N_2 adsorption-desorption isotherms and pore diameter graph (inset) of MA and BMMA.

FESEM analysis:

The FESEM images show a porous nature of the surface of both the materials. Round shaped depressions (~100 nm) with smaller pores (~10–15 nm) are observed in both the materials and the results so obtained are in good accordance with the previous analysis (Fig. 2).

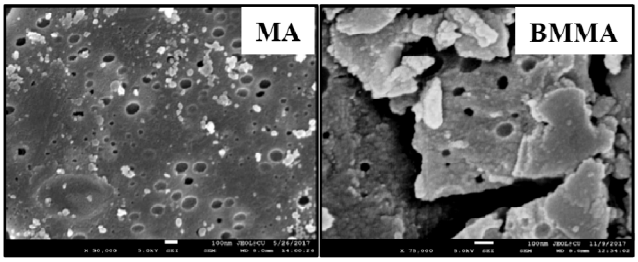

Fig. 2. FESEM images of MA and BMMA.

TEM analysis:

The particle size ~ 45 nm for MA and ~35 nm for BMMA were obtained from TEM images (Fig. 3).

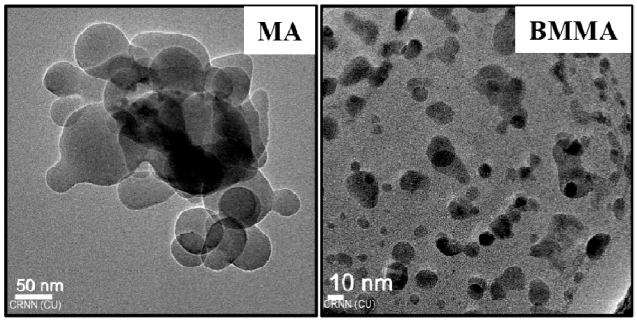

Fig. 3. TEM images of MA and BMMA.

FTIR analysis:

For MA, a peak at 746 cm^{-1} is found due to Al-O bond vibration. The modification by BCD moiety was confirmed in the BMMA material, by the peaks at 3469 cm^{-1} (due to O-H stretching vibration), 1637 cm^{-1} (due to O-H bending vibration), 867 cm^{-1} (due to C-H bending vibration) (Fig. 4). The functionalities of all the peaks are tabulated in Table 1.

Powder XRD analysis:

From this crystallographic technique we observed that, MA is crystalline in nature and obtained in γ phase. Whereas,

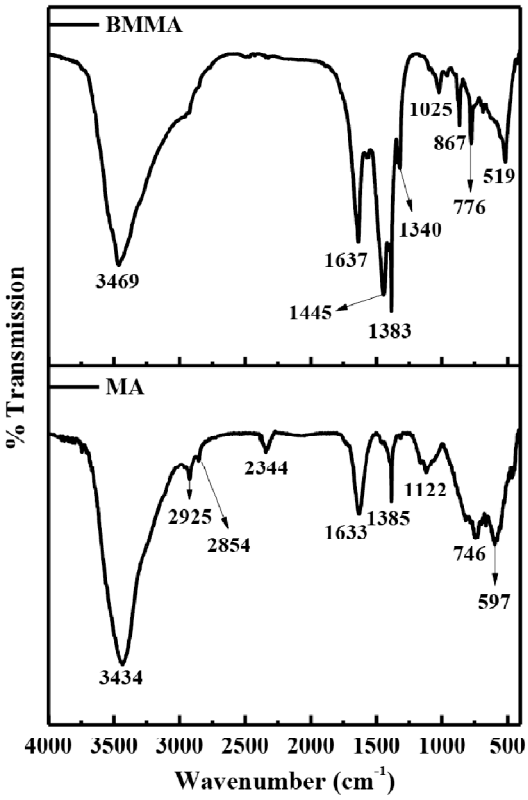

Fig. 4. FTIR spectra of MA and BMMA.

Table 1. IR spectral data of the prepared alumina nanoparticles with their possible functional groups

Peak position (cm^{-1})	Functionality
3469, 3434	O-H stretching vibration[25]
2925	Out-of-plane asymmetric vibration of $-CH_2$ group[26]
2854	Symmetric stretching of $-CH_2$ group[25]
2344	C-O stretching vibration of CO_2 group may get adsorbed from the atmosphere[27–29]
1637, 1633	O-H bending vibration[25]
1445, 1385, 1383, 1340	C-H bending vibration[26]
1122	Alcoholic C-O stretching vibration[26]
1025	Ring vibrations of cyclohexane ring of BCD molecule[26]
867	C-H bending vibration[30]
776, 746	Stretching vibration of Al-O bond[31,32]
597	Out-of-plane bending vibration of O-H bond[26]
519	In-plane bending vibration of O-C-O group[33]

the BMMA material is amorphous in nature and no major diffractions were obtained from its PXRD pattern (Fig. 5).

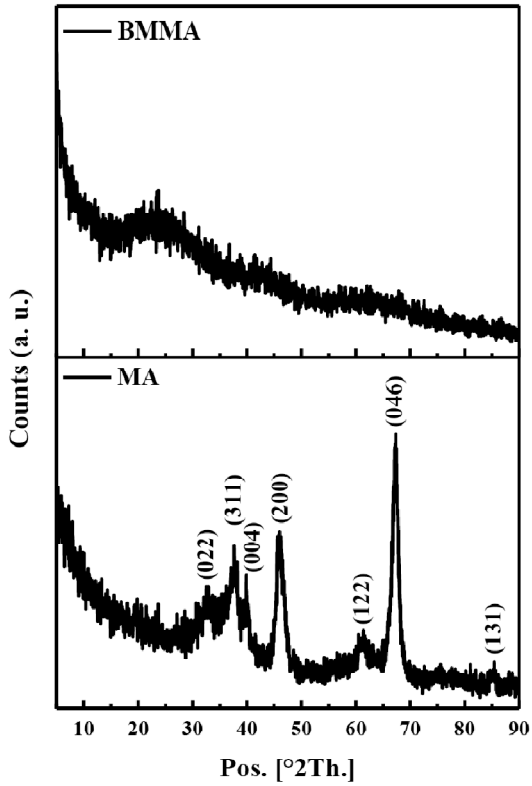

Fig. 5. PXRD patterns of MA and BMMA.

Cell viability test:

Cell viability test has been done by MTT assay with the provided two materials, MA and BMMA. From the findings of this experiment, it is clear that both MA and BMMA decreases the proliferation of HCT 116 cells and increases cell death. It has been observed that MA (IC_{50}: 15.61 ng/mL) has greater effect than BMMA (IC_{50}: 23.39 ng/mL) (Fig. 6). HEK 293 (Normal Human Epithelial Kidney) cells were also treated with MA and BMMA with same doses as for HCT 116 cells. Death percentage of HEK 293 cells at highest doses (for MA 35.68 ng/mL and for BMMA 56 ng/mL) were found to be 11.83% and 32.7% respectively (Fig. 7), whereas death percentage of HCT 116 cells were 88.24% for MA and 89.18% for BMMA. For confirmation of apoptosis, Annexin-V binding study was performed in presence or absence of MA for 24 h. 60.8% cells were apoptotic in 24 h (Fig. 8A and 8B). A table is made

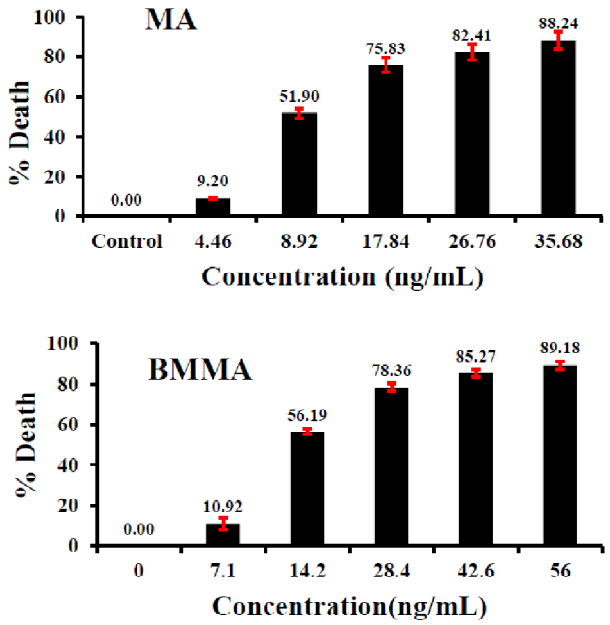

Fig. 6. HCT 116 cells (1×10^6 cells/mL) were treated with different concentrations of MA and BMMA for 24 h and viability were measured by MTT assay.

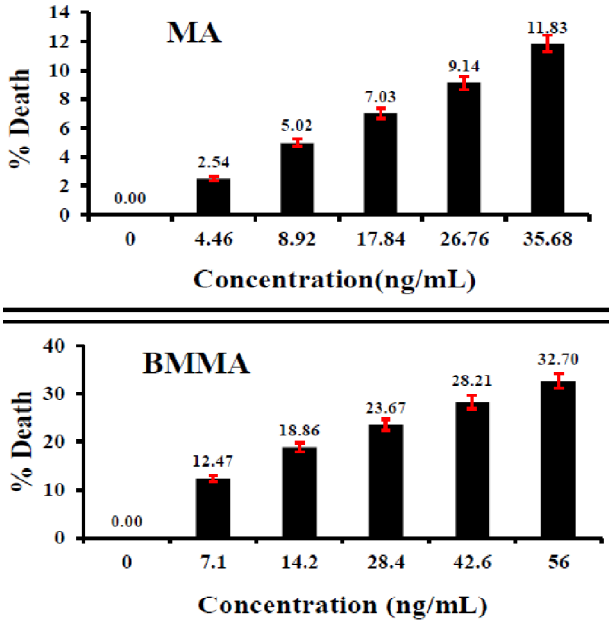

Fig. 7. HEK 293 cells (1×10^6 cells/mL) were treated with different concentrations of MA and BMMA for 24 h and viability were measured by MTT assay.

in order to compare the IC_{50} values of anticancer drugs to that of our work to have a quick idea (Table 2).

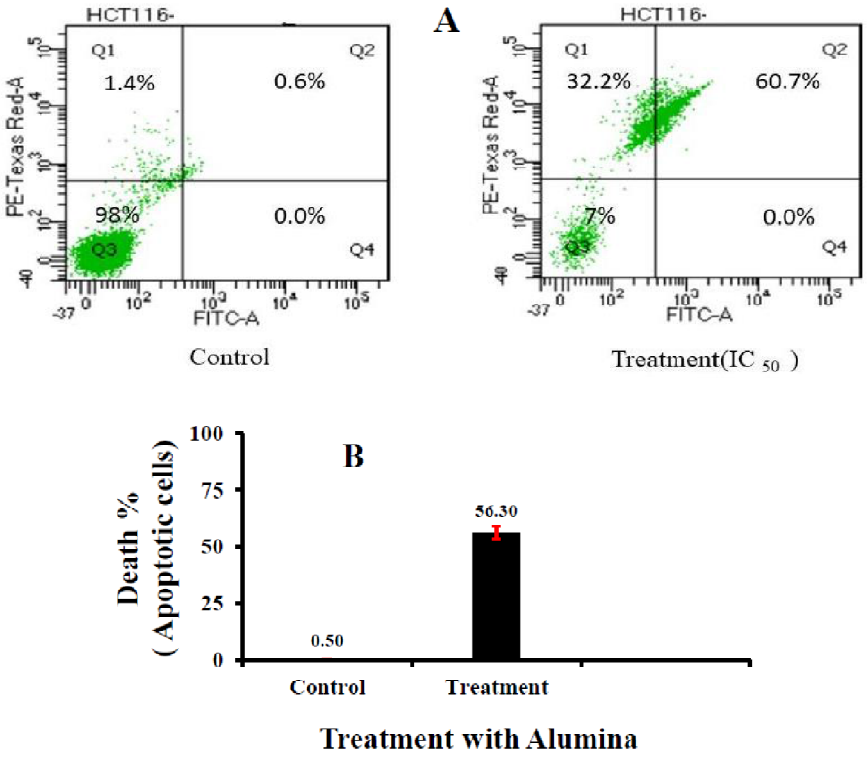

Fig. 8. HCT 116 cells were treated with IC_{50} (1×10^6 cells/mL) of MA for 24 h and apoptotic cells were measured by Annexin V-FITC/PI binding assay via FACS (8A and 8B). Results presented here are one of the three representative experiments (±S.D.).

Table 2. IC_{50} values of some reported colonic anticancer drug

Anticancer drug	Colon cancer cell line	IC_{50} (ng/mL)	References
5-Fluorouracil	HCT 116 cells	25860	34
Guttiferone K	HT-29 cells	3290	35
Flavopiridol	HCT 116 cells	16.87	36
Argentatin B	HCT-15	10950	37
	PC-3	15520	37
Cisplatin	HCT-15 and PC-3	4200	37
Sorafenib	HCT 116 cells	1390	38
MA	HCT 116 cells	15.61	This work
BMMA		23.39	

Cancer cell death is desired through apoptosis. Phosphatidyl serine (PS) present in the inner membrane of living cell is exposed to the outer membrane during cellular apoptosis. Annexin V can bind to this PS. When FITC (green fluorescence) conjugated Annexin V is added to apoptotic cells, it binds with PS and intensity of green fluorescence reflects % apoptotic cells. After passing through early- and late-apoptotic phases, cells become necrotic when membrane integrity is lost and sub-cellular organelles like DNAs are exposed in the system. Propidium iodide (PI) can bind with these exposed DNA and give red fluorescence whose intensity directly correlates with % of necrotic cells. FITC and PI negative cells are live cells. Thus adding mixture of FITC bound Annexin V and PI in cells, % of live cells, % early-apoptotic cells, % of late-apoptotic cells and % of necrotic cells are obtained through FACS analysis.

In our study, HCT 116 cells treated with or without of MA (IC_{50} : 15.61 ng/mL) for 24 h, showed 7% live cells (Q3), 0% early-apoptotic cells (Q4), 60.7% late-apoptotic cells (Q2), and 32.2% necrotic cells in contrast to 98% live cells in MA untreated cells (control) (Fig. 8A).

Possible mechanism:

It has been observed that ~52% of cell death in colon cancer cells occurs in presence of ~8.9 ng/mL of MA which is much higher as compared to BMMA, 7.1 ng/mL of which can cause ~11% cell death in a similar case. This observation of higher cytotoxity of MA towards colon cancer cells may be attributed to several reasons. The toxicity of metal

oxide especially aluminium oxide has already been proven by earlier researchers[11–13] which resulted in an electrostatic attraction between the metal oxide NPs and the surface of the cells. The metal oxide NPs can bind with the surface of the cells and dissociate into its ionic form and oxygen radicals. The interaction between the NPs and biomolecules present in the cells facilitate the dissociation of the NPs. For normal cells, the metal incorporation into the cell line by passive transport can support the cell development by ion supplement approach. The oxygen radical can be removed by the super oxide dismutase (SOD) and catalase enzymes. Therefore, the oxidative stress can be controlled. But for cancer cells, such enzymes may be insufficient or may not function properly and therefore the oxidative stress will increase with the NPs concentration. The enhanced metal ion concentrations inhibit the growth of the cancer cells by binding with essential biomolecules present in the cell[10,39–41]. In case of BMMA, the release of Al^{3+} in the cellular medium becomes hindered due to the presence of BCD molecules in the environment resulting in lesser production of oxygen free radicals also. Therefore the resultant toxicity of BMMA towards colon cancer cells becomes less as compared to the MA.

The result of cytoxicity of the materials towards the cell line of normal kidney cells is just the reverse. 8.92 ng/mL of MA can cause ~5% cell death in HEK 293 cells while 7.1 ng/mL of BMMA can cause 12.47% cell death. The higher toxicity of BMMA towards HEK 293 cell line compared to MA can be explained on the basis of the special interactions of BCD with kidney cells. The smaller size and amorphous nature of the BMMA material helps the NPs to penetrate the cell membrane more easily and interact with the cellular components to cause cellular damage[10]. BCD is reported to cause increase in apical vacuolation and formation of giant lysosomes in kidney cells followed by disruption in mitochondria and other cell organelles to cause cellular damage[42]. These features dominate the protection of BCD towards breakdown of alumina in causing toxicity and become more toxic particularly towards normal kidney cells.

Conclusion

In the present work we have reported the preparation of pristine and modified mesoporous alumina in an acidic environment taking pluronic F-68 as a surfactant and aluminium isopropoxide as a source of alumina. Both of the materials were then thoroughly characterized using different analytical tools. Finally, we tried to study the toxicity of such materials towards cancer (HCT 116) and normal (HEK 293) cell lines. The results were quite interesting and agreeable with the literature reports. We also estimated the percentage amount of live, early, late-apoptosis and necrosis cells if the HCT 116 cells were treated with IC_{50} amount of MA. Overall the cell toxicity of both MA and BMMA is higher towards cancer cells (~89%) with 36 and 56 ng/mL concentrations respectively than that of normal cells (~12% and 32% respectively) with same concentrations of the materials. The developed materials therefore have good potential to be used for disruption of cancer cells.

Acknowledgement

Pritam Singh is very gratefull to the University Grants Commission (UGC) (Ref. No. 20/12/2015(ii)EU-V dated 24.08.2016) for providing necessary fellowship. We are also thankful to Mr. Nayan Ranjan Saha, Department of Chemical Technology, University of Calcutta, India for PXRD.

References

1. M. Alem, A. Tarlani and H. R. Aghabozorg, *RSC Adv.*, 2017, **7**, 38935.
2. P. Singh and K. Sen, *J. Porous Mater.,* 2017, **25**, 965.
3. S. A. El-Safty, Y. Kiyozumi, T. Hanaoka and F. Mizukami, *Mater. Lett.,* 2008, **62**, 2950.
4. S. A. El-Safty, M. A. Shenashen, M. Ismael and M. Khairy, *Adv. Funct. Mater.,* 2012, **22**, 3013.
5. P. Zeng, *Mater. Sci. Technol.*, 2008, **24**, 505.
6. Y. C. Rajan, B. S. Inbaraj and B. H. Chen, *RSC Adv.*, 2015, **5**, 15126.
7. X. Ke, T. Huang, R. Dargaville, Y. Fan, Z. Cui and H. Zhu, *Sep. Purif. Technol*., 2013, **120**, 239.
8. S. C. Sahu and A. W. Hayes, *Toxicol. Res. App*., 2017, **1**, 1.
9. A. Derbalah, M. Shenashen, A. Hamza, A. Mohamed and S. E. Safty, *IJARBS*, 2017, **4**, 68.
10. Y. -W. Huang, M. Cambre and H.-J. Lee, *Int. J. Mol. Sci*., 2017, **18**, 2702.
11. H. Bahadar, F. Maqbool, K. Niaz and M. Abdollahi, *Iran. Biomed. J.*, 2016, **20**, 1.
12. L. Chen, R. A. Yokel, B. Henning and M. Toborek, *J. Neuroimmune. Pharmacol*., 2008, **3**, 286.
13. A. A. Alshatwi, P. V. Subbarayan, E. Ramesh, A. A. Al-Hazzani, M. A. Alsaif and A. A. Alwarthan, *J. Biochem. Molecular. Toxicol*., 2002, **26**, 469.

14. G. Tiwari, R. Tiwari and A. K. Rai, *J. Pharm. Bioall. Sci.*, 2010, **2**, 72.
15. H. Rachmawati, C. A. Edityaningrum and R. Mauludin, *AAPS Pharm. Sci. Tech.*, 2013, **14**, 1303.
16. S. Baboota and S. P. Agarwal, *Indian J. Pharm. Sci.*, 2002, **64**, 408.
17. B. Abdous, S. M. Sajjadia and L. Ma'mani, *J. Appl. Biomed.*, 2016, **15**, 210.
18. R. Zhang, L. Li, J. Feng, L. Tong, Q. Wang and B. Tang, *ACS Appl. Mater. Interfaces*, 2014, **6**, 9932.
19. P. F. Fulvio, R. I. Brosey and M. Jaroniec, *ACS Appl. Mater. Interfaces*, 2010, **2**, 588.
20. M. Thommes, K. Kaneko, A. V. Neimark, J. P. Olivier, F. Rodriguez-Reinoso, J. Rouquerol and K. S. W. Sing, *Pure Appl. Chem.*, 2015, **87**, 1051.
21. P. Singh and K. Sen, *Colloid Polym. Sci.*, 2018, **296**, 1711.
22. A. Vinu, M. Miyahara, V. Sivamurugan, T. Mori and K. Ariga, *J. Mater. Chem.*, 2005, **15**, 5122.
23. A. M. Putz, A. Len, C. Ianăşi, C. Savii and L. Almásy**,** *Korean J. Chem. Eng.*, 2016, **33**, 749.
24. Z. A. ALOthman, *Materials*, 2012, **5**, 2874.
25. S. Gupta, P. C. Ramamurthy and G. Madras, *Polym. Chem.*, 2011, **2**, 221.
26. J. Coates and R. A. Meyers, 2016, **12**, (Ed.) 10815.
27. M. Sanati and A. Andersson, *J. Mol. Catal.*, 1993, **81**, 51.
28. S. Kannan, *Int. J. Curr. Microbiol. App. Sci.*, 2014, **3**, 341.
29. H.-Z. Yu, S. Ye, H.-L. Zhang, K. Uosaki and Z.-F. Liu, *Langmuir*, 2000, **16**, 6948.
30. C. A. Contreras, S. Sugita and E. Ramos, *AZo J. Mater.*, 2006, **8**, 122.
31. J. M. Saniger, *Mater. Lett.*, 1995, **22**, 109.
32. N. Fuloria and S. Fuloria, Publisher: Studium Press India Pvt. Ltd., 2013.
33. M. A. Subhan, P. Sarker and T. Ahmed, *J. Sci. Res.*, 2014, **6**, 553.
34. G. Pan, T.-T. Jia, Q.-X. Hunag, Y.-Y. Qiu, J. Xu, P.-H. Yin and T. Liu, *Colloids Surf. B: Biointerfaces*, 2017, **159**, 375.
35. W. L. T. Kan, C. Yin, H. X. Xu, G. Xu, K. K. W. To, C. H. Cho, J. A. Rudd and G. Lin, *Int. J. Cancer*, 2013, **132**, 707.
36. V. Smith, F. Raynaud, P. Workman and L. R. Kelland, *Mol. Pharmacol.*, 2001, **60**, 885.
37. E. Alcántara-Flores, A. E. Brechú-Franco, P. García-López, L. Rocha-Zavaleta, R. López-Marure and M. Martínez-Vázquez, *Molecules*, 2015, **20**, 21125.
38. T. Mazard, A. Causse, J. Simony, W. Leconet, N. Vezzio-Vie, A. Torro, M. Jarlier, A. Evrard, M. D. Rio, E. Assenat, P. Martineau, M. Ychou, B. Robert and C. Gongora, *Mol. Cancer Ther.*, 2013, **12**, 2121.
39. S. Andra, S. K. Balu, J. Jeevanandham, M. Muthalagu, M. Vidyavathy, Y. S. Chan and M. K. Danquah, *Naunyn-Schmiedeberg's Arch. Pharmacol.*, 2019.
40. D. L. Jonesa and L. V. Kochian, *FEBS Lett.*, 1997, **400**, 51.
41. C. Exley and J. D. Birchall, *J. Theor. Biol.*, 1992, **159**, 83.
42. V. J. Stella and Q. He, *Toxicol. Pathol.*, 2008, **36**, 30.